Article

Current Biology

Deficient synaptic neurotransmission results in a persistent sleep-like cortical activity across vigilance states in mice

Graphical abstract

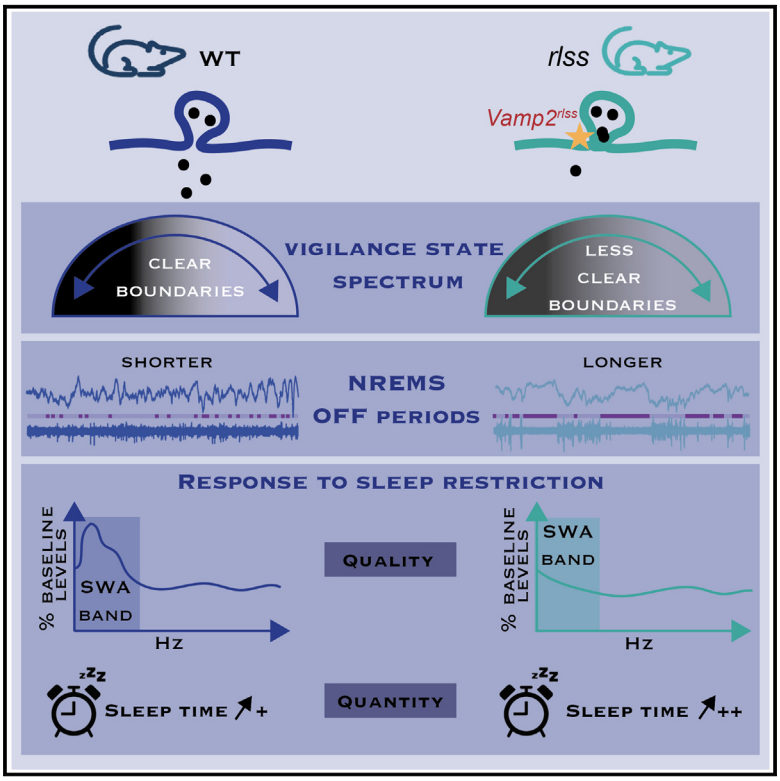

Highlights

- Altered neurotransmission (*Vamp2*^{rlss}) leads to longer periods of neuronal silence
- Spectral signatures of vigilance states are less distinct in *rlss* mice
- Neuronal dynamics during NREM sleep in *rlss* mice are reminiscent of anesthesia
- Sleep pressure marker changes after sleep deprivation are attenuated in *rlss* mice

Authors

Mathilde C.C. Guillaumin, Christian D. Harding, Lukas B. Krone, ..., Patrick M. Nolan, Stuart N. Peirson, Vladyslav V. Vyazovskiy

Correspondence

mathilde.guillaumin@ndcn.ox.ac.uk (M.C.C.G.), vladyslav.vyazovskiy@dpag.ox.ac.uk (V.V.V.)

In brief

Using a mouse model of altered neurotransmission (*Vamp2*^{rlss}), Guillaumin et al. show that differences typically observed between vigilance states in neural dynamics and spectral signatures can be markedly reduced. The findings support the idea that synaptic function and neuronal excitability are direct contributors to sleep-wake architecture.

Guillaumin et al., 2025, Current Biology *35*, 1716–1729
April 21, 2025
https://doi.org/10.1016/j.cub.2025.02.053

CellPress

CellPress
OPEN ACCESS

Current Biology

Article

Deficient synaptic neurotransmission results in a persistent sleep-like cortical activity across vigilance states in mice

Mathilde C.C. Guillaumin,[1,2,3,12,*] Christian D. Harding,[3,4,5] Lukas B. Krone,[3,4,5,6] Tomoko Yamagata,[1,3,4] Martin C. Kahn,[3,4,5] Cristina Blanco-Duque,[3,4,5] Gareth T. Banks,[7] Peter Achermann,[8] Cecilia Diniz Behn,[9,10] Patrick M. Nolan,[7] Stuart N. Peirson,[1,3,4] and Vladyslav V. Vyazovskiy[3,4,5,11,*]

[1]Nuffield Department of Clinical Neurosciences, University of Oxford, John Radcliffe Hospital, Oxford OX3 9DU, UK
[2]Medical Research Council Brain Network Dynamics Unit, Nuffield Department of Clinical Neurosciences, University of Oxford, Mansfield Road, Oxford OX1 3TH, UK
[3]Sir Jules Thorn Sleep and Circadian Neuroscience Institute (SCNi), University of Oxford, South Parks Road, Oxford OX1 3QU, UK
[4]Kavli Institute for Nanoscience Discovery, University of Oxford, South Parks Road, Oxford OX1 3QU, UK
[5]Department of Physiology, Anatomy and Genetics, University of Oxford, Parks Road, Oxford OX1 3PT, UK
[6]University Hospital of Psychiatry and Psychotherapy, University of Bern, Hochschulstrasse 6, Bern 3012, Switzerland
[7]Mammalian Genetics Unit, MRC Harwell Institute, Harwell Science and Innovation Campus, Didcot OX11 0RD, UK
[8]Institute of Pharmacology and Toxicology, University of Zürich, Winterthurerstrasse 190, Zürich 8057, Switzerland
[9]Department of Applied Mathematics & Statistics, Colorado School of Mines, 1301 19th Street, Golden, CO 80401, USA
[10]Department of Pediatrics, University of Colorado Anschutz Medical Campus, 13001 East 17th Place, Aurora, CO 80045, USA
[11]X (formerly Twitter): @VVyazovskiy
[12]Lead contact
*Correspondence: mathilde.guillaumin@ndcn.ox.ac.uk (M.C.C.G.), vladyslav.vyazovskiy@dpag.ox.ac.uk (V.V.V.)
https://doi.org/10.1016/j.cub.2025.02.053

SUMMARY

Growing evidence suggests that brain activity during sleep, as well as sleep regulation, are tightly linked with synaptic function and network excitability at the local and global levels. We previously reported that a mutation in synaptobrevin 2 (*Vamp2*) in restless (*rlss*) mice results in a marked increase of wakefulness and suppression of sleep, in particular REM sleep (REMS), as well as increased consolidation of sleep and wakefulness. In this study, using finer-scale *in vivo* electrophysiology recordings, we report that spontaneous cortical activity in *rlss* mice during NREM sleep (NREMS) is characterized by an occurrence of abnormally prolonged periods of complete neuronal silence (OFF-periods), often lasting several seconds, similar to the burst suppression pattern typically seen under deep anesthesia. Increased incidence of prolonged network OFF-periods was not specific to NREMS but also present in REMS and wake in *rlss* mice. Slow-wave activity (SWA) was generally increased in *rlss* mice relative to controls, while higher frequencies, including theta-frequency activity, were decreased, further resulting in diminished differences between vigilance states. The relative increase in SWA after sleep deprivation was attenuated in *rlss* mice, suggesting either that *rlss* mice experience persistently elevated sleep pressure or, alternatively, that the intrusion of sleep-like patterns of activity into the wake state attenuates the accumulation of sleep drive. We propose that a deficit in global synaptic neurotransmitter release leads to "state inertia," reflected in an abnormal propensity of brain networks to enter and remain in a persistent "default state" resembling coma or deep anesthesia.

INTRODUCTION

Despite recent advances in our understanding of neurophysiological and molecular mechanisms of sleep-wake control, it remains unclear how sleep and wake alternation is regulated at a brain-wide scale and whether such fundamental aspects of neuronal function as synaptic release have a role to play in that respect.

The restless (*rlss*) mouse line, obtained via a forward genetics sleep screen and possessing a mutation in synaptobrevin 2/*Vamp2* (a gene encoding the key synaptic-release machinery protein VAMP2), showed an array of sleep and behavioral phenotypes,[1] including a decreased amount of NREM sleep (NREMS) in the dark phase, alongside an overall decrease in REM sleep (REMS) time. More strikingly, the number of sleep and wake episodes and of state transitions was markedly reduced in *rlss* mice, correlating with an increased duration of episodes in all vigilance states compared with littermate controls. The probability to transition from one state to the next in normal conditions was found to be markedly reduced in *rlss* mice, leading to a general "vigilance state inertia."

The mutation in *Vamp2* results in markedly decreased neurotransmitter release probability in *rlss* mice, altering synaptic transmission.[1] These findings raised several questions regarding

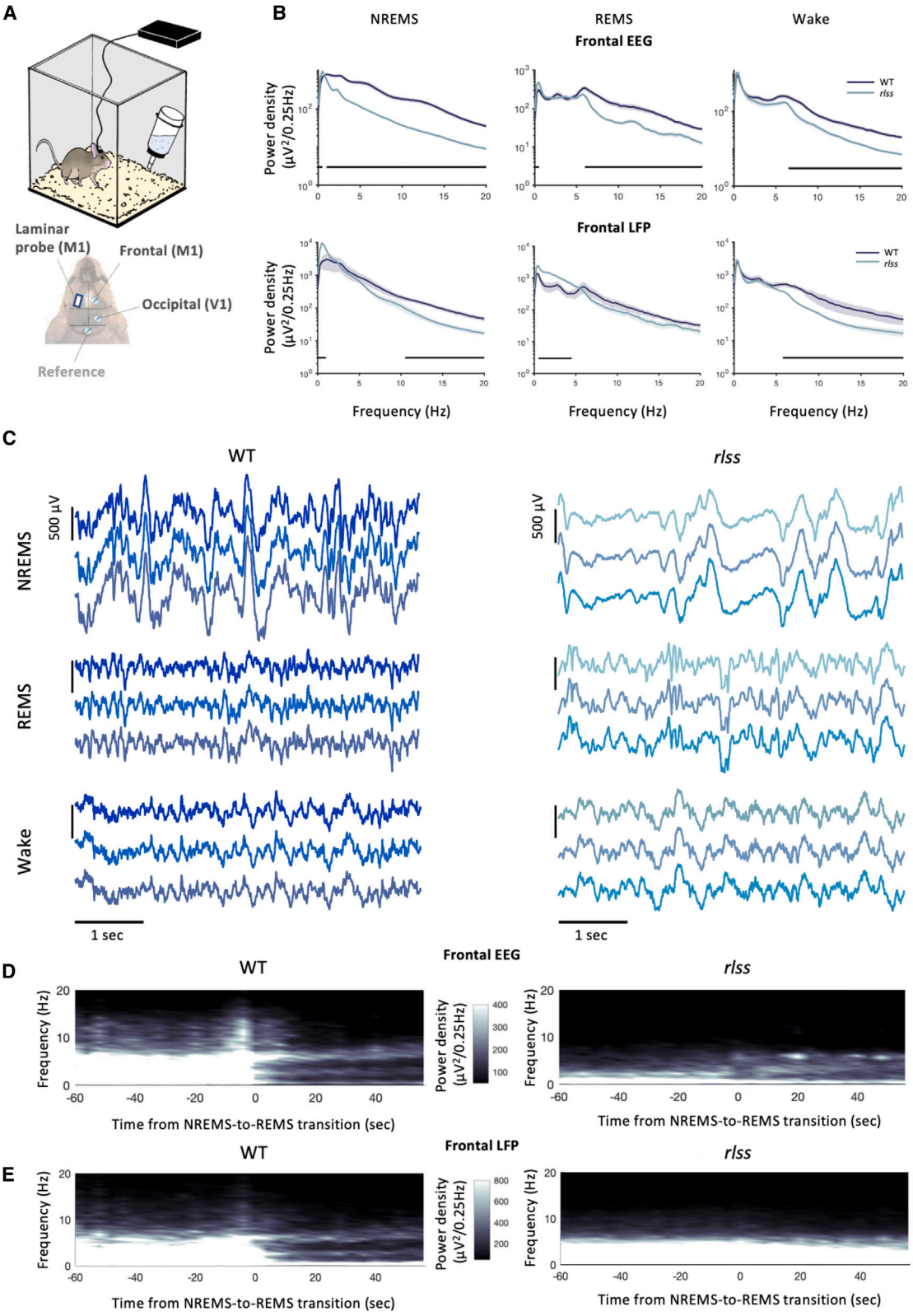

(legend on next page)

the impact that *rlss* phenotypical traits impose on the electrophysiological signatures of vigilance states, on sleep quality, and on the accumulation of sleep pressure during wake. In short, having shown changes in the architecture of vigilance states,[1] we now take a different approach and look at the "quality" of the states themselves to address the question of whether changes in state dynamics and architecture between *rlss* and wild-type (WT) mice induce qualitative differences between states.

Electroencephalogram (EEG) slow-wave activity (SWA), which corresponds to the EEG power in the slow-wave frequency range (0.5–4 Hz) in NREMS, has been a useful measure to evaluate sleep-wake dynamics. Slow waves tend to dominate the EEG during NREMS and can be recorded across the entire cortical surface.[2,3] Both animal and human studies have shown that SWA levels are closely linked to sleep-wake history, where SWA levels at the onset of NREMS positively correlate with preceding time spent awake and levels subsequently decrease during NREMS.[4,5] SWA has therefore been traditionally used as a marker of sleep pressure.[6,7] However, EEG captures global signals across the cortical surface. Local field potentials (LFPs) and multi-unit activity (MUA) instead provide insight into sleep-wake dynamics at a more local level. In addition, as the initiation of slow waves (depth-positive/surface-negative deflections) corresponds to periods of neuronal silence,[3,8–13] which also depend on the levels of network synchrony,[12] MUA allows us to investigate the underlying patterns of neuronal silence ("OFF-periods").[13]

In the present study, we used EEG, LFP, and MUA recordings, combined with sleep deprivation (SD) and auditory stimulation paradigms, to gain a better understanding of the sleep depth of *rlss* mice. Auditory stimuli are commonly used to investigate sleep depth, sensory dissociation during sleep, and arousal thresholds from NREMS and REMS.[14–18] We investigated the spectral signature of global sleep and wake states, in particular at state transitions. We further explored the neuronal dynamics underlying the marked behavioral changes observed and, using a mathematical model of sleep regulation,[19,20] we examined the homeostatic regulation of sleep in *rlss* mice. We found that, in *rlss* mice, the boundaries between electrophysiological signatures of vigilance states were less distinct than in control animals and that sleep homeostasis dynamics were altered, with *rlss* mice being slower to dissipate accumulated sleep pressure. This was not, however, associated with an altered responsiveness to external sensory stimuli such as a sound.

This study suggests that impaired neurotransmitter release leads to an increased propensity to gravitate toward a "default state" of cortical activity,[21–28] with important consequences for global and local sleep architecture and sleep homeostasis.

RESULTS

rlss mice show increased propensity for hybrid states of vigilance

Using EEG in freely moving mice from the motor (M1) and visual (V1) cortical areas, combined with LFP recordings from M1 (Figure 1A), we found that *rlss* mice have higher spectral power in the very low frequencies in NREMS and REMS and less power in the higher frequency bins in REMS (EEG only), NREMS, and wake (Figures 1B and S1A). Interestingly, the differences between *rlss* and WT mice's spectral signatures diverged between the frontal EEG and LFP signals in REMS, with an increase in the very-low delta band and theta (and higher) frequencies in the frontal REMS EEG and an increase in the upper delta band in the frontal LFP in *rlss* mice compared with WT mice (Figure 1B, middle). Changes in the EEG occipital derivation paralleled the ones observed in the frontal EEG (Figure S1A); therefore, as LFP signals were recorded from M1, we also focused on EEG signals from this region (frontal). Local cortical dynamics thus revealed a disparity between local intracortical and brain surface ("global") signatures of REMS in *rlss* mice.

LFP signals in *rlss* mice were also characterized by a decreased amplitude, especially during NREMS, when traces were reminiscent of burst suppression patterns typically observed during general anesthesia but also coma, hypothermia, and some early infantile pathologies[29–32] (Figure 1C; Video S1). Such EEG/LFP signatures across vigilance states indicate that sleep inertia not only means fewer state transitions in *rlss* mice[1] but also an intrusion of default-mode-like traits[21] across all states of vigilance, with the well-known spectral signatures of NREMS, REMS, and wake being affected. The boundaries between states' typical signatures appear less distinct in *rlss* mice due to an increased power in the very slow frequencies—not only in NREMS but also in REMS and wake—associated with a decreased theta power in REMS in *rlss* mice. At a finer time resolution, looking at spectrograms at the transitions from NREMS to REMS, we found marked differences between *rlss* and WT mice. Blurred boundaries between states in *rlss* mice appeared all the more evident, with the drop in spectral power in the slow-frequency range (0.5–4 Hz) that is usually observed at NREMS-to-REMS transitions being significantly reduced in *rlss* mice (Figures 1D and 1E).

rlss mice show prolonged periods of neuronal silence across all vigilance states and especially during NREMS, reminiscent of burst suppression patterns

These EEG and LFP results raised the following question: what features in the brain activity of *rlss* mice contribute to such sleep

Figure 1. *rlss* mice show an increased level of similarity between vigilance state signatures

(A) Schematic of recording setup. M1, primary motor cortex; V1, primary visual cortex.

(B) Frontal EEG (upper) and LFP (lower) power spectra during NREMS, REMS, and wake in WT and *rlss* mice. Black bars at the bottom indicate the frequency bins for which the power is significantly different ($p < 0.05$) between WT and *rlss* mice. Values shown as mean ± SEM. See also Figure S1A.

(C) Examples of LFP traces from three channels from a WT mouse (left) and *rlss* mouse (right) during NREMS, REMS, and wake. The different colors indicate different channels.

(D) Evolution of the power spectra (spectrograms; time-frequency plots) in the frontal EEG at NREMS-to-REMS transitions averaged across WT (left) and *rlss* (right) mice. Time 0: onset of REMS.

(E) As in (D) but for LFP signals. Note that here n(WT) = 3.

Unless otherwise stated, n(WT) = 5 and n(rlss) = 5.

CellPress
OPEN ACCESS

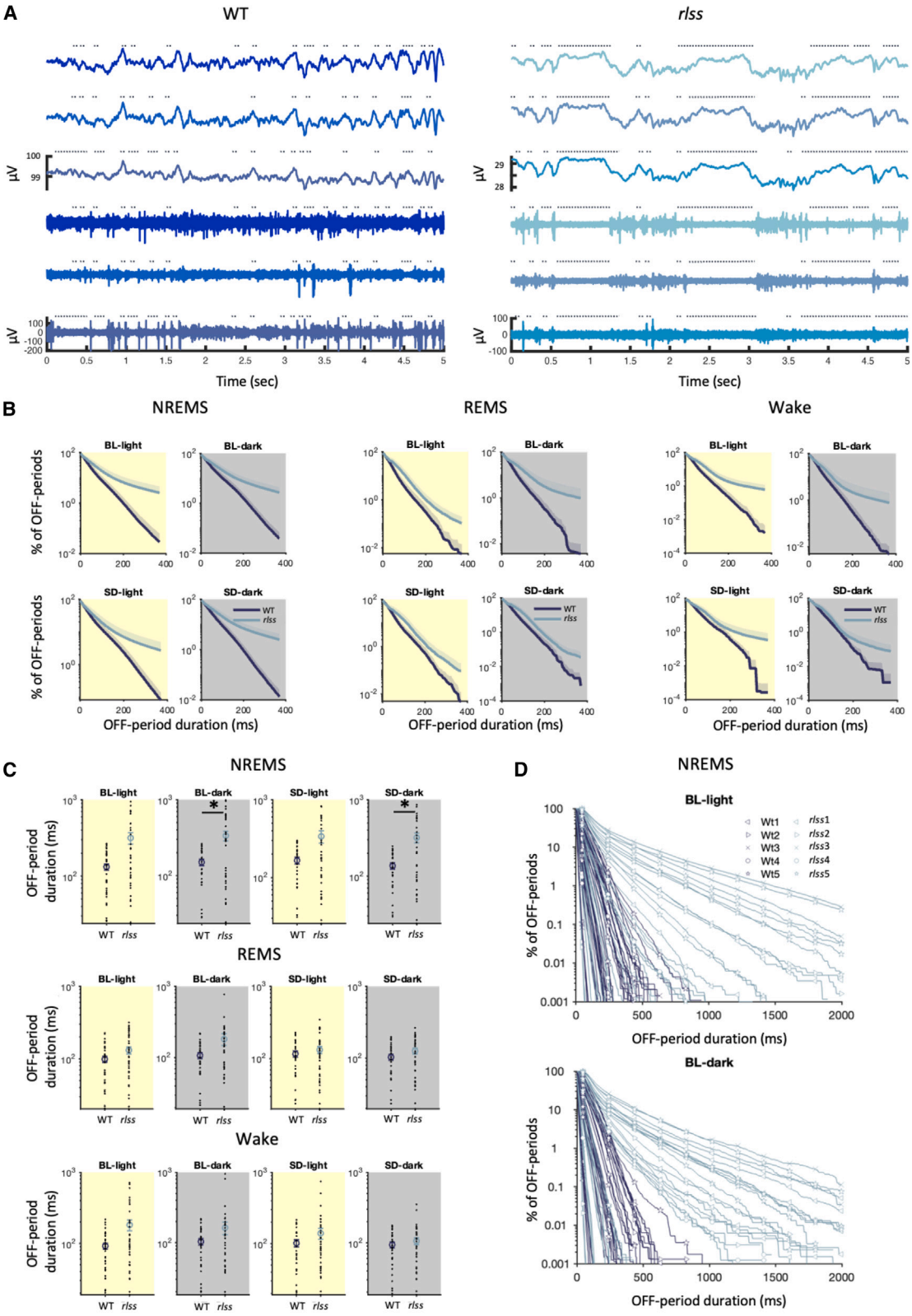

Figure 2. *rlss* mice show prolonged periods of neuronal silence across vigilance states that are reminiscent of burst suppression patterns

(A) Examples of three LFP (upper traces) and corresponding MUA (lower traces) signals in a WT mouse (left) and *rlss* mouse (right) during 5 s of NREMS. Dotted lines indicate location of OFF-periods, as detected by the algorithm (see STAR Methods), with no threshold applied.

(legend continued on next page)

architecture and spectral variations? Using MUA recordings and our recently developed "ON/OFF-period" detection algorithm[13] (Figures 2, S2, and S3), we discovered that neuronal firing in *rlss* mice ceases for seconds at a time during NREMS, in a locally synchronized manner (Figures 2A and S2; Video S1). Compared with WTs, in *rlss* animals, periods of such synchronized neuronal silence (OFF-periods) lasted significantly longer and coincided with very low-amplitude, nearly isoelectric EEG and LFP traces (Figures 2A, 2B, and S2; Video S1). Importantly, this also held true in REMS and wake when OFF-periods were generally longer in *rlss* mice (Figure 2B). Long OFF-periods were not detected in all channels; however, all of the *rlss* mice and none of the WT mice have at least one channel presenting with much longer OFF-periods (Figures 2D and S2C). For ON-periods, we did not find a significant difference in their average length between genotypes (Figure S3B). Similarly, we found no significant difference in ON-period spike density between WT and *rlss* mice (Figure S3C).

Next, we specifically investigated the longest OFF-periods, selecting the 5% longest OFF-periods (see STAR Methods). We found that OFF-periods are significantly longer in *rlss* mice, with the longest ones being about twice as long as in WT during NREMS (Figures 2B and 2C); this further supports a state of "neuronal inertia," whereby in *rlss* mice neurons are less likely to resume activity upon a period of silence of a certain duration. To quantify this further, we performed a linear fit to the survival curves for each mouse and channel in the baseline (BL) light phase (Figures 2D and S2C) and computed the average slope (see STAR Methods). We found that, for fits to the entire survival curve, there was no difference in slopes between WT and *rlss* ($F(1,68) = 1.8$, $p = 0.184$). However, for fits to the part of the survival curve associated with longer OFF-periods, the slopes for *rlss* were shallower than the slopes for WT. This held for OFF-periods with durations greater than 65 ms ($F(1,68) = 4.03$, $p = 0.0488$), and the difference in slopes became more pronounced as the duration threshold increased (e.g., for a threshold of 200 ms, $F(1,68) = 7.99$, $p = 0.0062$, see STAR Methods). Additionally, a Levene's test indicated that variances were different ($p = 3.37e{-}04$), with greater variability for the *rlss* mice. This greater variability was also confirmed when comparing the difference between groups in the variance of the longest OFF-period durations across channels recorded in a given mouse (Figure S2B).

Firing rates detected from MUA were not significantly altered in *rlss* mice (Figure S1B), but we observed an increased uniformity in their vigilance state spectral characteristics, particularly striking at state transitions (Figures 1B, 1D, and 1E). When looking at inter-spike intervals (ISIs), we see a decrease in the number of short ISIs during both NREMS and REMS in *rlss* mice and an increase in the number of long ISIs during NREMS only (Figure S1C). This suggests an inertia at the cellular level during sleep in *rlss* mice, with active-to-silent state transitions at the cellular and network levels lagging behind global state transitions, as was indeed visible in firing rate dynamics around state transitions (Figures S4A–S4C).

Given a "neuronal" inertia that may underlie the less clear-cut boundaries between vigilance state signatures and the alterations in EEG and LFP spectra, notably in the slow-wave frequency range—which is traditionally used to investigate sleep homeostasis dynamics—we next asked whether sleep homeostasis was affected in *rlss* mice.

Sleep homeostasis is generally conserved in *rlss* mice, with increased sleep quantity, but not sleep quality, in response to SD

To investigate the sleep homeostatic response in *rlss* mice, we subjected the mice to a 6-h SD protocol starting at light onset (time/Zeitgeber 0, ZT0), after which the mice were left undisturbed for the subsequent 18 h. Following this 6-h SD period, *rlss* mice showed a markedly decreased sleep latency compared with WT littermates (Figure 3A). This is the only case when we observed state switching probability being higher in *rlss* mice than WTs. Time spent in NREMS in the 6 h following SD was increased by 1 h in *rlss* animals compared with WTs, whereas REMS time was halved (Figures 3B–3D). However, across the whole recovery period (18 h post SD), BL comparative sleep structure was restored, with *rlss* mice spending less time in both NREMS and REMS than WTs (Figures 3B–3D, right). At the end of this 18-h recovery period, both WT and *rlss* mice had reached their BL daily levels of REMS and had mostly caught up on NREMS (Figures 3B and 3C).

We found that the relative increase in SWA commonly triggered by SD was markedly reduced in *rlss* mice (Figures 3E and S6B). This was the case for both EEG and LFP signals and was particularly marked in the 2 h directly following SD (Figures 3E, 3F, and S6B). This may indicate that, although sleep homeostasis is partly conserved in *rlss* mice (time taken to reach BL levels of NREMS and REMS is comparable between genotypes, Figures 3B and 3C), SWA, reflecting sleep pressure, might not build up at the same rate in *rlss* mice. To summarize, *rlss* mice

(B) Survival curves of OFF-periods (relative to their duration) in NREMS (left), REMS (middle), and wake (right) during a baseline (BL) day (upper) and a sleep deprivation (SD) day (lower), separately for the light and dark phases of a 24-h day in WT and *rlss* mice. The graphs show on the y axis (log-scale) what % of OFF-periods have a duration greater than or equal to the corresponding x axis value. Values shown as mean + SEM.

(C) Average OFF-period durations of the 5% longest OFF-periods during NREMS (upper), REMS (middle), and wake (lower) in a BL (left) or SD day (right), separately for the light and dark phases. Values shown as mean ± SEM, with black dots indicating individual channels. Wilcoxon rank sum test; $^*p < 0.05$. NREMS BL-dark: $p = 0.0326$, rank sum = 741; NREMS SD-dark: $p = 0.0229$, rank sum = 731. Note that if running those statistics with a repeated-measures ANOVA to take into account mouse dependency, we obtain: NREMS BL-dark: $p = 0.0222$ ($F(1,7) = 8.561$), NREMS SD-dark: $p = 0.0348$ ($F(1,7) = 6.8233$).

(D) Percentage of periods of neuronal silence ("OFF-periods") longer than a given duration (x axis) for all individual channels of *rlss* (light blue curves, *n*(mice) = 5) and WT mice (dark blue curves, *n*(mice) = 5). BL conditions during the light and dark phases. Only NREMS is considered here. Each animal is coded with a different symbol (x, o, etc.), showing how all *rlss* mice have at least one channel in the upper right-hand corner of the graphs (prolonged OFF-periods), unlike any of the WT mice.

See also Figures S1B–S1D, S2, and S3, and Video S1.

n(WT) = 5 (4 beyond BL-L phase) with resp. 6, 10, 6, 7, and 6 channels in each mouse (total = 35 channels), *n*(rlss) = 5, with resp. 9, 6, 8, 5, and 7 channels in each mouse (total = 35 channels). BL, baseline; SD, sleep deprivation.

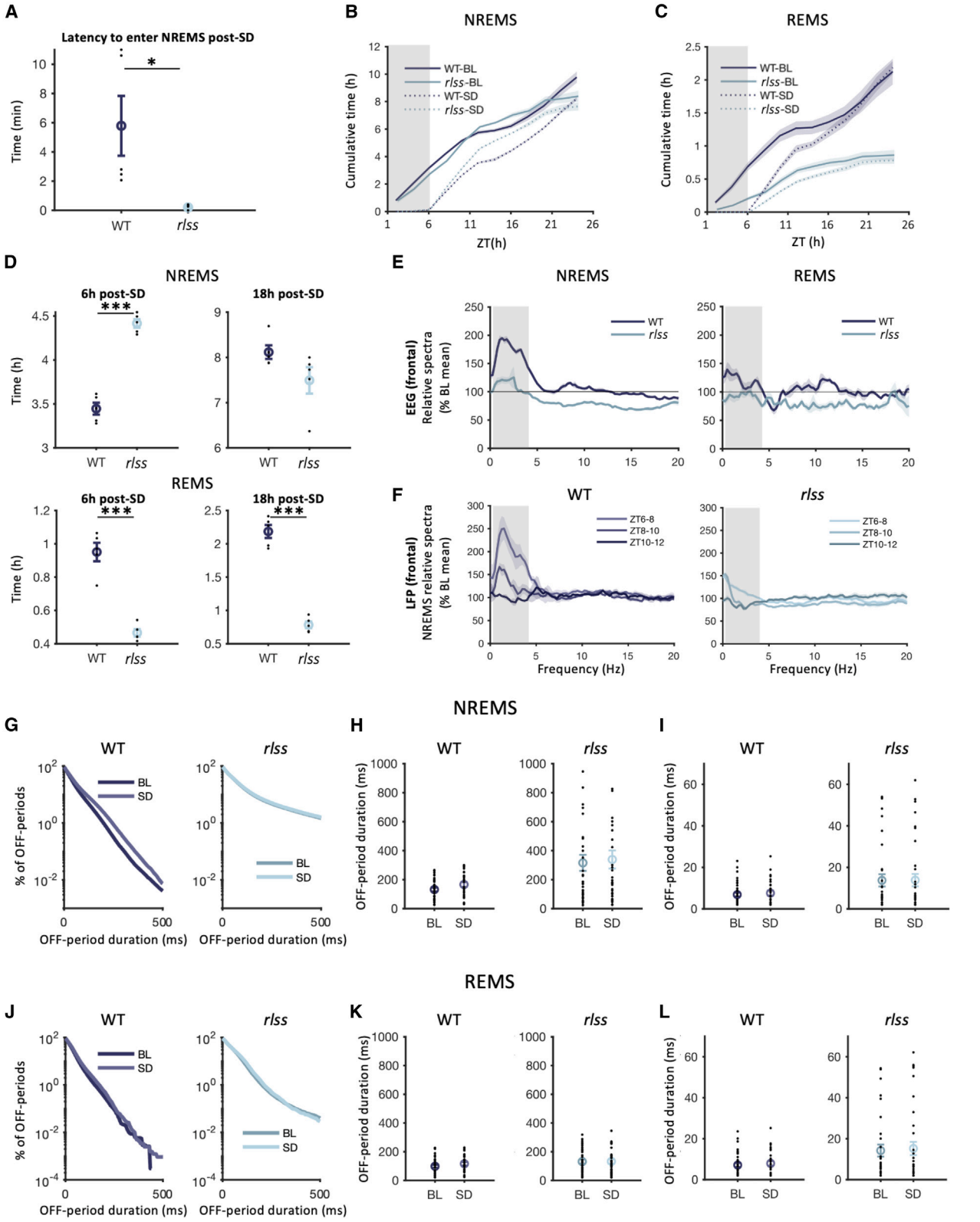

(legend on next page)

are able to compensate for sleep loss in a similar amount of time to WTs (Figures 3B and 3C), but this is made possible by spending more time asleep (Figure 3D), as overall SWA is lower compared with WTs and their increase in SWA during recovery NREMS (which allows for sleep pressure dissipation) is lower compared with their own BL levels (Figures 3E, 3F, and S6B). In short, there seems to be a trade-off between sleep quantity (duration spent sleeping) and sleep quality (higher SWA levels) in those mice following an SD challenge.

We observed that OFF-period durations following SD did not increase in *rlss* mice but nor did they in WTs (Figures 3H and 3I). This can be expected, as changes in the average duration of OFF-periods naturally occur between BL and SD conditions in WTs[12]; therefore, genotype-specific changes may be more easily observable in terms of incidence (Figure 3G) than duration. Another explanation is that we analyzed the longest OFF-periods and combined early and late sleep. Yet, early sleep usually contains longer OFF-periods than later sleep.[12,33] No significant change in OFF-period duration in REMS was observed in either WT or *rlss* mice in response to SD (Figures 3J–3L).

The dampened increase in SWA in *rlss* mice compared with WTs following SD may arise from *rlss* mice experiencing chronically elevated sleep pressure, thus leaving less capacity for a further increase in response to SD. Alternatively, it may be that, as the neural activity of *rlss* mice persistently gravitates toward a "default state," they do not accumulate sleep pressure as steeply as WTs during waking.[20] To investigate this, we used an adapted version of the "two-process model" of sleep regulation that we previously described.[19]

To investigate the dynamics of SWA and sleep homeostasis in *rlss* mice, we applied the adapted version of the two-process model of sleep regulation[19,34] to recordings obtained in *rlss* and WT mice (Figure 4A). We performed two sets of optimizations, using 24 h of BL only or using 24 h of BL followed by an SD day (see STAR Methods). When comparing the results obtained with both approaches (BL only vs. BL + SD day), we found that the parameter values obtained with either approach were similar overall, except when optimizations were run using LFP data (Figure 4B). *rlss* mice had similar rise rates of process S (rs) values but significantly reduced values of gain constant (gc, the rate of decrease of S) and S_U (upper asymptote of S/SWA levels) in both EEG derivations (Figure 4B, upper and middle panels) but not LFP (Figure 4B, lower panels). Thus, sleep pressure decreases (gc) more slowly in *rlss* mice compared with WTs. Interestingly, because the upper threshold (S_U) for process S is lower in *rlss* mice, these mice reach BL levels of sleep as fast as WT mice (Figures 3B and 3C) despite this slower dissipation of sleep pressure.

Conserved behavioral reaction to auditory stimuli, but altered response at the neuronal level, in *rlss* mice

Finally, given the inertia shown by *rlss* mice to switch between certain states, both at the behavioral and neuronal levels, we asked whether their response to external stimuli—such as a sound—was impaired too. We wanted to address whether the elevated power in the slow-wave range and the smaller increase in SWA following SD could reflect a higher sleep depth in *rlss* mice, which would lead to a higher arousal threshold. Using an auditory stimulation paradigm (Figure 5A), we found that the number of full arousals (i.e., the mouse stays awake for at least 16 s after the sound, see STAR Methods) following the sounds was similar across genotypes, but there were significantly fewer brief arousals (<16 s) in *rlss* mice (Figure 5C). This may reflect, once again, the state inertia previously described in those mice,[1] whereby once *rlss* mice have entered a state they tend to remain in that state for longer than WTs, hence the lower likelihood of a brief arousal (if the mouse does wake up, then it stays in that state longer as it cannot switch back to NREMS as easily). This hypothesis is further supported by the occurrence of brief awakenings (short arousals $\leq$16 s) during NREMS, which is three times less likely in *rlss* mice during undisturbed (BL) recordings (Figure 5B). Of note, the number of muscle twitches in response to the sound was similar across genotypes ($F(1,7) = 0.002$, $p = 0.967$, Figure 5C, right), indicating no obvious impairment in acute motor or EEG response to environmental triggers (Figure 5F).

When looking at the EEG spectra during the sound (8 s) and during segments of the same length either before or after the

Figure 3. Response to sleep deprivation reveals a decreased sleep quality that is compensated for by an increase in sleep quantity in *rlss* mice

(A) Latency to enter NREMS following a 6-h SD protocol.
(B) Cumulative time spent (in 2-h bins) in NREMS in WT and *rlss* mice during a BL or SD day. Highlighted in gray is the SD period for the SD day only.
(C) As in (B) for REMS.
(D) Amount of time spent in NREMS (top) or REMS (bottom) during the 6 h (left) or 18 h (right) protocol, following a 6-h SD protocol in WT and *rlss* mice.
(E) Frontal EEG spectra in NREMS (left) and REMS (right) relative to the baseline mean in WT and *rlss* during the 2 h following a 6-h SD protocol. Delta frequency band (0.5–4 Hz) highlighted in gray.
(F) LFP spectra in NREMS relative to baseline mean in WT (left) and *rlss* (right) mice in the 6 h following a 6-h SD protocol, separated in 2-h blocs. Delta frequency band (0.5–4 Hz) highlighted in gray.
(G) Survival curves of OFF-periods (relative to their duration) occurring during NREMS during the light phase of a BL and SD day in WT (left) and *rlss* (right) mice.
(H) Average OFF-period duration of the 5% longest OFF-periods in NREMS in the light phase of a BL and SD day in WT (left) and *rlss* (right) mice. Black dots indicate individual channels.
(I) As in (H) but for the 5% shortest OFF-periods.
(J) As in (G) but for OFF-periods occurring during REMS.
(K) As in (H) but for OFF-periods occurring during REMS.
(L) As in (I) but for OFF-periods occurring during REMS.
See also Figures S3A–S3C, S4, and S6.
Values shown as mean ± SEM, with black dots indicated individual values (mice in A and D or channels in H, I, K, and L). *n*(WT) = 5 (3 for LFP-derived parameters), *n*(rlss) = 5. WT mice: resp. 6, 10, 6, 7, and 6 channels in each mouse (total = 35 channels); rlss mice: resp. 9, 6, 8, 5, and 7 channels in each mouse (total = 35 channels). Independent samples t tests in (A) and (D); $^{*}p < 0.05$, $^{***}p < 0.001$. BL, baseline; SD, sleep deprivation; ZT, zeitgeber time.

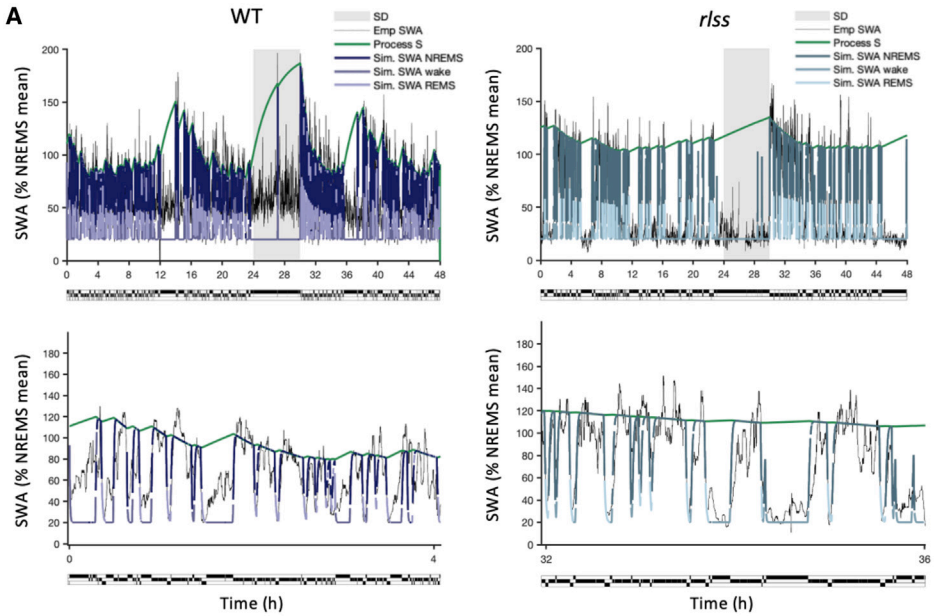

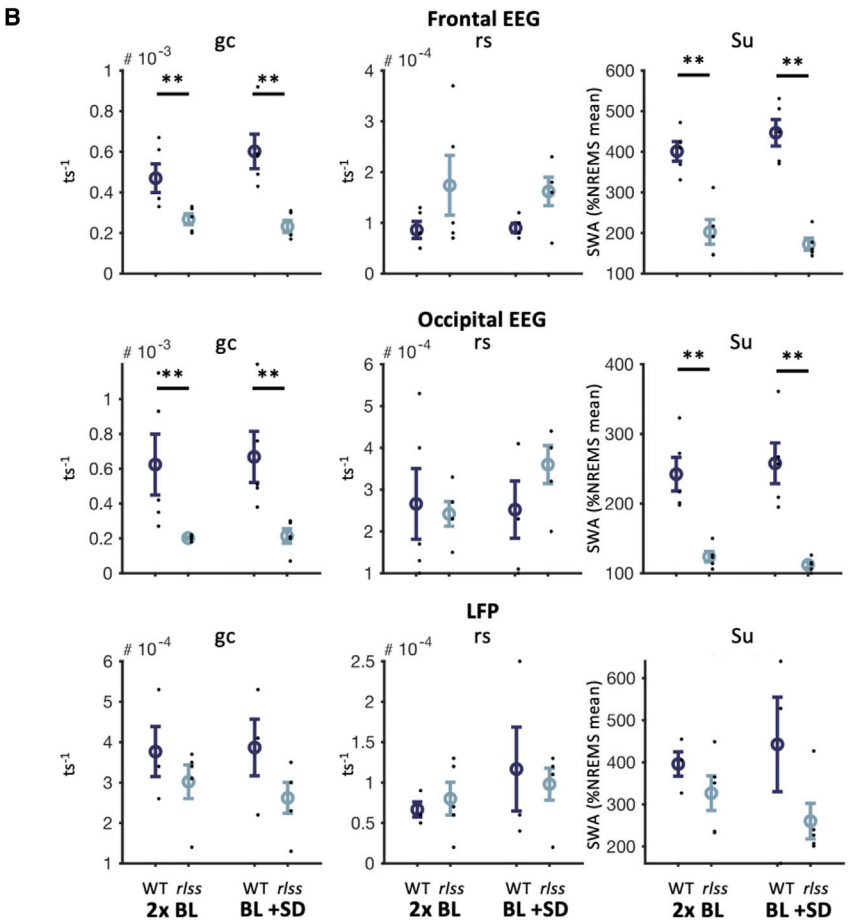

(legend on next page)

sound, we found a significant difference between genotypes in NREMS ($F(1,7) = 19.309$, $p = 0.003$) and REMS ($F(1,7) = 12.359$, $p = 0.010$) and a significant time point × genotype interaction if the sound started during NREMS ($F(2,14) = 5.431$, $p = 0.018$) but not during REMS ($F(2,14) = 1.395$, $p = 0.280$) (Figure 5E). Specifically, the change in the EEG spectra in response to the sound was more pronounced in WTs than *rlss* mice when mice were originally in NREMS before being woken up.

Thus, *rlss* mice show a conserved arousal threshold (comparable number of full arousals and twitches in both genotypes). Yet, as following SD, it appears that *rlss* mice show a "rigidity" in their neuronal dynamics so that the scope for variation (as measured by spectral power) across states and wake/sleep experiences is markedly reduced. But the link between arousal threshold and sleep depth is not straightforward, especially in *rlss* mice for which brain oscillations are affected. As mentioned above, NREMS SWA has often been considered a marker of sleep pressure—reflecting sleep-wake history—and also sleep depth (which can also be evaluated by assessing arousal thresholds). When subdividing trials, considering those when the sound started during NREMS (Figures 5G, S5A, and S5B) or REMS (Figures S5C–S5E), we find that the response to the sound (i.e., arousal threshold), as measured by the level of electromyogram (EMG) during the sound, has no evident correlation with pre-sound SWA levels, except in the occipital EEG when the sound started in NREMS (Figure 5G), this effect being significant in WT mice only and being small (adjusted R^2(WT) = 0.015).

DISCUSSION

rlss mice are characterized by a mutation in the VAMP2 SNARE protein that induces a change at the molecular scale by impairing neurotransmitter release.[1] Our results therefore support the idea that sleep regulation is tightly linked to synaptic function. In particular, we show that *rlss* mice display long periods of neuronal silence—strikingly reminiscent of deep anesthesia—that underlie increased SWA during BL conditions but lead to an inability to fully adapt neural dynamics to behavioral experiences such as SD or auditory stimuli. Mathematical modeling revealed that the rate of sleep-pressure dissipation is slower in those mice. Finally, we found this "neural rigidity" is compensated for by global behavioral states, such as increased sleep time in response to SD.

An impairment in the "sleep switch"?

Our previous findings,[1] combined with the auditory stimulation results described here, support the idea of "vigilance state inertia" in *rlss* mice. The decrease in neurotransmitter-release efficiency leads to a difficulty in switching between consecutive vigilance states. Previous studies have suggested a mechanism for a sleep/wake switch in both flies and rodents.[35,36] "Flip-flop" switches have been proposed, either to control the transitions between REMS and NREMS[37] or to allow rapid transitions between NREMS and wake and prevent lingering between two vigilance states—half awake and half asleep.[36,38] Saper et al.[38] propose that, if neuronal firing is weakened on either side of this bistable switch, then the stability of the switch is compromised; on the other hand, they also propose that the time to transition from one state to the next may depend on the ability of a population of neurons that promote a given state to overcome the "resistance" of the population of neurons promoting the current state.[36] In *rlss* mice, we observe an increased stability of each state, both at the behavioral and cellular levels. Concomitantly, we see more similar spectral signatures between vigilance states. This indicates that, should a sleep-switch exist, not only is it not transitioning between states as readily in those mice but also that it is "leaky," staying halfway between states, resulting in mixed states with characteristics of both sleep and wake.

Another mouse line (*Sleepy*), developed using a forward genetics approach, exhibited increased NREMS time; the gain-of-function mutation present in these mice affected the *Sik3* gene, leading to a shorter SIK3 protein kinase, which is likely involved in the intracellular signaling mediating regulation of sleep amount.[39–41] Interestingly, despite this hypersomnia in contrast to *rlss* mice, NREMS delta power was increased in *Sleepy* mice just as in *rlss* mice. *Sleepy* mice showed an exaggerated response to SD, suggesting an increased inherent sleep need despite an increased delta power during BL wake. The ability of *Sleepy* mice to stay awake when exposed to arousal-promoting stimuli was conserved, showing that, as with *rlss* mice, their ability to be awake should the need arise is not impaired.[39]

An important point is whether the decreased state-transitioning probability observed in *rlss* mice signifies that it is uniformly difficult for them to switch to another state or, rather, that one state is at a stronger disadvantage. In particular, because of the NREMS-like features of wake and REMS in *rlss* mice it may be less relevant for them to enter full NREMS. And, indeed, when looking at state-transitioning probabilities from Banks et al.,[1] we observe an absolute 44% change in probability to transition between wake and NREMS (wake->NREMS: 34% decrease, NREMS->wake: 10% increase) and a 16% change in probability to transition from REMS to NREMS (REMS->NREMS: 87% decrease, NREMS->REMS: 71% decrease). The REMS->wake transitions are relatively less affected (absolute 8% decrease). Although this would need to be further tested, these results are in line with the hypothesis that rather than a state inertia, those mice might be gravitating toward a "default state" mode[21–26,42] regardless of their vigilance state, thus making it less relevant to spend time in NREMS.

Figure 4. Sleep homeostasis dynamics are altered in *rlss* mice, with a lower decay rate of sleep pressure

(A) Upper: example of empirical and simulated slow-wave activity (SWA) across 48 h (24 h of baseline + 6-h sleep deprivation + 18-h recovery) in an example WT (left) and *rlss* (right) mouse. Lower: zoomed-in inserts (see x axis values) of a 4-h section from the corresponding upper panels. Colors indicate the corresponding vigilance state, also shown underneath each panel as a hypnogram.

(B) Model parameters (gc, gain constant determining decay of S; rs, rise rate of S; Su, upper asymptote of S) when modeling the SWA levels of the frontal EEG signal (upper), occipital EEG (middle), and LFP (lower), using 2 BL days (left panels of each parameter) or a BL + SD day (right panels of each parameter), in WT ($n = 5$ for EEG, $n = 3$ for LFP) and *rlss* mice ($n = 5$). Values shown as mean ± SEM; black dots indicate individual values. Non-parametric Mann-Whitney tests; $^{**}p < 0.01$. ts = 4 s epoch (time unit used for simulations), $ts^{-1} = 1/4$ s.

CellPress
OPEN ACCESS

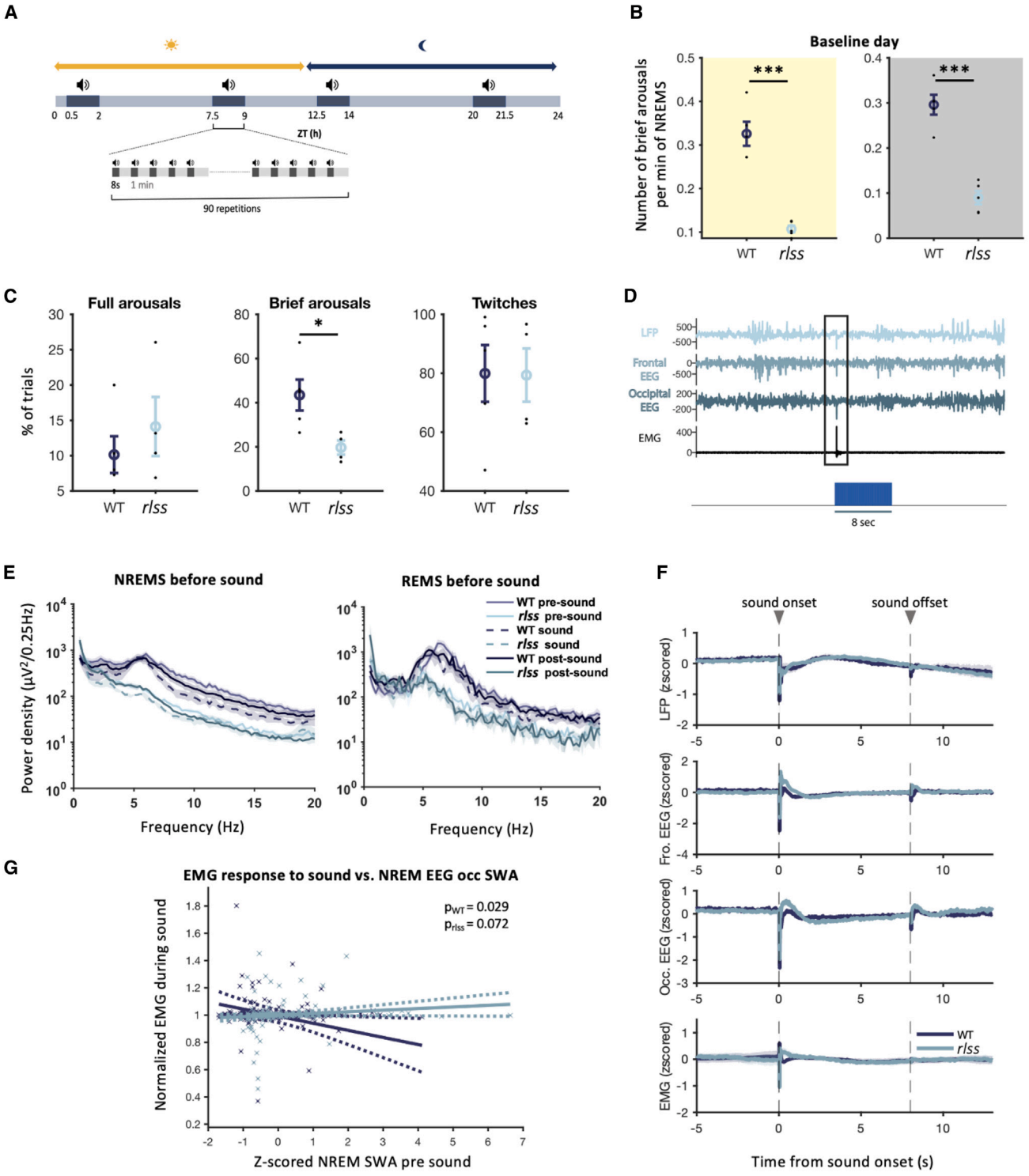

Figure 5. *rlss* mice show a conserved arousal threshold but an impaired neuronal response to an auditory stimulus during sleep

(A) Schematic of experimental design.

(B) Number of brief arousals per minute of NREMS during the light and the dark phase of a baseline day. Two-way ANOVA with within-subject factor: LD phase, between-subject factor: genotype. We found a significant main effect of genotype ($F(1,8) = 79.783$, $p < 0.001$), with no main effect of LD phase ($F(1,8) = 2.783$, $p = 0.134$) and no significant interaction LD phase × genotype ($F(1,8) = 0.194$, $p = 0.671$). Post hoc testing with Bonferroni correction for multiple comparisons revealed that, in the light phase, there was a significant difference between *rlss* and WT mice ($p < 0.001$), with a similar result in the dark phase ($p < 0.001$).

(C) Proportion of sound stimulation events resulting in full arousals, brief arousals, and muscle twitches. Independent samples t tests.

(legend continued on next page)

Higher sleep pressure or a higher propensity to return to a default state?

The shorter sleep time in BL conditions in *rlss* mice raises the question of whether they have higher sleep efficiency (dissipating sleep pressure faster), a decreased sleep-pressure buildup during waking, or whether they live under elevated sleep pressure. The two-process model of sleep regulation, which predicts the evolution of process S, is a useful tool to address this question. A study in humans comparing short sleepers and long sleepers found that both groups had the same constants of increase and decrease of process S, implying that short sleepers may live under a higher sleep pressure.[43] This hypothesis was further supported by a computational study simulating habitual short and long sleep.[44] Here, we find *rlss* mice have similar rising rate of S but significantly lower rates of decrease and a significantly lower upper asymptote of S. These results may indicate that instead of having an inherently elevated sleep pressure (which their lower S upper asymptote argues against), *rlss* mice may have a higher propensity to enter or approach a "default state."

There is evidence that cortical oscillations are not merely an epiphenomenon or simply a substrate for sleep-related processes to occur (e.g., memory consolidation) but have a role in vigilance state control and sleep regulation.[45] Thus, if the cortex keeps track of the accumulation of sleep need, then the persistent sleep-like patterns we observe in our cortical recordings could indicate a partial sleep debt discharge across both sleep and waking states.

Impaired vesicular release leads to longer neuronal OFF-periods

Our MUA recordings revealed striking neuronal firing patterns in *rlss* mice during NREMS. Slow waves were associated with prolonged periods of neuronal silence, where neighboring neurons stop firing in a coordinated manner for prolonged periods of time, with the longest OFF-periods being about twice as long in *rlss* mice as in WT mice (Figure 2). While prolonged OFF-periods appear to be a distinctive feature of cortical neuronal activity in *rlss* mice, a marked interchannel variability in their OFF-period dynamics was also noted (Figures 2D and S2). This may be explained by changes in the overall network excitability due to the mutation in *Vamp2*, leading some neurons to fire in an untimely way in some channels, interrupting the synchronous OFF-periods observed across other channels.

Those periods of neuronal silence resulted in very-low amplitude LFP signals. Such patterns of neuronal activity are seldom seen during natural sleep and are a more common feature of GABA-mediated general anesthesia.[46,47] It would be of great interest to further evaluate whether those changes observed in *rlss* mice are accompanied by deviations in infra-slow modulations in OFF-periods occurrence within individual NREMS episodes.

We have previously described an impairment in vesicular release in *rlss* mice due to the mutation in *Vamp2*, which plays a key role in vesicular and cellular membrane fusion.[1] *rlss* mice showed a marked decrease in vesicular-release probability following single action potentials. An impairment in vesicular release could lead to a state akin to anesthesia. Indeed, it has been shown that general anesthetics, such as isoflurane, propofol, or etomidate, induce a decrease in synaptic neurotransmitter release machinery by interacting with multiple SNARE proteins.[48,49] This could account for the long periods of neuronal silence observed in *rlss* mice while they are (spontaneously) asleep: given their mutation leading to a structural change in VAMP2, which is a SNARE protein, *rlss* mice may present features of an "inherently anesthetized" state.

Interestingly, it was previously shown that injection of the $GABA_A$ agonist muscimol led to a catalepsy-like state followed by a hyperactive state in mice, with the EEG of both of those states displaying a shift in power toward lower frequencies.[50] This is strikingly similar to our findings, with increased cortical synchrony in all states and reduced power in high frequencies, alongside a hyperactive phenotype. The authors propose that the effects of muscimol point toward a crucial role for inhibitory connections in slow-wave synchronization. Thus, our results suggest that the decreased vesicular release is in many ways akin to increased inhibitory tone. The physiological sleep of *rlss* mice is in several ways more similar to non-physiological states, such as cataplexy or anesthesia (e.g., with an inefficiency to properly dissipate sleep pressure), than normal sleep.

Switching between anesthesia and wake

Studies in Drosophila suggest that switching between states requires a tightly regulated excitatory and inhibitory balance between neuronal populations.[51–53] Additional evidence indicates that the reversible loss of consciousness caused by anesthetics occurs via the arousal and sleep pathways,[54] with the mechanisms underlying sleep homeostasis and anesthesia overlapping.[55–59] Yet, these observations often start from the premise that sleep and wake are mutually exclusive states between which animals switch in a clear-cut manner, which is now acknowledged to be more complex.[60] Indeed, as clearly shown

(D) Example of a muscle twitch and associated artifacts in the LFP and EEG channels in response to a sound (y axes: μV).
(E) Power density spectra calculated from the occipital EEG in the 8 s before, 8 s during, and 8 s after a sound, if the sound onset occurred during NREMS (left) or REMS (right).
(F) LFP (1 representative channel per mouse), frontal EEG, occipital EEG and EMG around sounds. Signals are extracted from all sound trials occurring during the light phase, and *Z* scored before being averaged across trials and across mice.
(G) Correlation between SWA (power in the 0.5–4 Hz frequency band) in the occipital EEG calculated over the 8 s before sound onset, and the average EMG levels during the 8-s sound. SWA is *Z* scored across all trials for a given mouse. EMG is normalized for each trial, independently, over the period starting 8 s before the sound onset, until sound onset. Only sound trials occurring when the mouse was in NREMS before the sound started are included. Each dot represents one sound trial in one mouse. Full line is the result of a linear regression. Dotted lines are the 95% confidence intervals from the linear regression (MATLAB "fitlm" function, WT: adjusted $R^2 = 0.015$, rlss: adjusted $R^2 = 0.011$).
See also Figures S4D, S4E, and S5.
n(WT) = 5 (3 for LFP), *n*(rlss) = 4. Values shown as mean ± SEM; black dots indicate individual values. $^*p < 0.05$, $^{***}p < 0.001$. Fro., frontal; Occ., occipital; ZT, zeitgeber time.

by several studies,[50,61,62] states may be viewed on a continuum, with some feature overlap. This is what we see in *rlss* mice, with an intrusion of NREMS-like features in REMS and wake states. It is remarkable that *rlss* mice display only mildly impaired cognitive and behavioral phenotypes typical of wakefulness,[1] despite profound alterations in brain activity. Just as in the occurrence of slow waves or decreased neuronal activity, which have been previously described in waking and not only in sleep,[63–65] our findings support that vigilance states are not necessarily separate phenomena with unambiguous boundaries but can share characteristics. Such overlapping features may fluctuate depending on specific waking behavior,[65] chemical manipulations,[61] or genetic alterations.[39]

Finally, the mutation affecting *rlss* mice being ubiquitous, two important questions arise, namely whether the observed changes in neuronal dynamics only occur in the cortex or also in other areas of the brain and whether the changes in vigilance state switching are mostly governed by cortical modifications. Future recordings from other cortical areas and other brain regions will allow further investigation of these questions. Of note, however, is that we have previously shown that the cortex plays a crucial role in vigilance state control and regulation.[45] Interestingly this study used a mouse model in which a subset of cortical-layer-5 neurons were silenced via an ablation of SNAP 25. The latter is one of the SNARE protein partners with which VAMP2 interacts for vesicular fusion.[66] This suggests that the changes in our mice could at least in part be governed by cortical changes. However, this does not rule out that synaptic transmission changes in subcortical areas may also play a role.

Conclusion

This combination of *in vivo* and computational work provides new insights into the mechanisms underlying sleep architecture and the alternation between vigilance states as well as the generation of slow waves. The preserved ability of *rlss* mice to respond to salient external stimuli suggests that neuronal dynamics and sleep-wake architecture can be markedly altered before leading to a phenotype that would represent an evolutionary disadvantage. Our findings represent a shift in the way states of vigilance and consciousness may be classified and support the idea that global synaptic function and neuronal excitability are direct contributors to sleep-wake architecture. Previous literature has focused on an increasing number of specific cell populations or brain subregions, which are thought to control the switch between well-defined states, but it may be that state control is more nuanced.[67] The possibility that states are controlled in a global manner, which we previously proposed,[45] has been overlooked, and, here, we suggest to shift the emphasis to the role of top-down control. Our findings regarding the mixed spectral signatures across states in *rlss* mice support the idea that wake and sleep are not homogeneous states but stand on a continuum of many possible states between full arousal and a profound coma, such as typical for deep anesthesia. We posit that a finely tuned global neuronal excitability allows the brain to transition quickly and seamlessly between a variety of states, while remaining around a sleep-like state toward which network activity always gravitates, by default, in the absence of stimulation.

RESOURCE AVAILABILITY

Lead contact

Further information and requests for resources and reagents should be directed to and will be fulfilled by the lead contact, Vladyslav V. Vyazovskiy (vladyslav.vyazovskiy@dpag.ox.ac.uk).

Materials availability

This study did not generate new unique reagents.

Data and code availability

Scripts and data used in this study can be accessed from "https://github.com/vladvyazovskiy/rlss." Any additional information required to re-analyze the data reported in this paper is available from the lead contact upon request.

ACKNOWLEDGMENTS

We thank Prof. Irene Tracey for stimulating discussions and valuable suggestions regarding data interpretation. We also thank Dr. Laura E. McKillop for valuable advice on surgical procedures. M.C.C.G. was supported by a BBSRC DTP grant (BB/J014427/1), a Swiss National Science Foundation grant (no. 310030_189110), and a Clarendon Fund Scholarship from the University of Oxford. C.D.H. was supported by funding from the Engineering and Physical Sciences Research Council (EPSRC, EP/S515541/1). L.B.K. was supported by a Wellcome Trust PhD studentship (203971/Z/16/Z) and by a Mann Senior Scholarship in medical sciences at Hertford College, Oxford. T.Y. was supported by the Naito Foundation (grant for studying overseas), a Uehara Memorial Foundation (postdoctoral fellowships for research abroad) and a Wellcome Trust Senior Investigator award (106174/Z/14/Z). M.C.K. was supported by a Berrow Foundation Lord Florey Scholarship. C.B.-D. was supported by a Wellcome Trust PhD studentship (109059/Z/15/Z) and a Clarendon Fund Scholarship from the University of Oxford. P.M.N. was supported by the MRC (grant codes MC_U142684173 and MC_UP_1503/2). S.N.P. was funded by the BBSRC (BB/ I021086/1) and a Wellcome Trust strategic award (098461/Z/12/Z). V.V.V. was funded by a John Fell OUP research fund grant (131/032), a Wellcome Trust strategic award (098461/Z/12/Z), and by Medical Research Council (UK) grant MR/S01134X/1.

AUTHOR CONTRIBUTIONS

M.C.C.G. performed implantation surgeries, experiments and data collection, data analysis, and writing of the manuscript and figures and acquired funding support; C.D.H. developed the OFF-period detection algorithm; L.B.K. contributed to the development of the OFF-period detection algorithm and advised on implantation, microlesions, and histology; T.Y. advised on surgeries and auditory stimulation protocol; M.C.K. advised on technical issues; C.B.-D. advised on methodology and data analysis for the auditory stimulation experiment; G.T.B. and P.M.N. assisted in the development of the mouse model and initial phenotyping of the *rlss* mice; P.A. advised on modeling methodology, simulation, and analyses and provided feedback on the manuscript; C.D.B. advised on methodology, contributed to the OFF-period analysis, and provided feedback on the manuscript; S.N.P. advised on study design, methodology, and supervision and acquired funding support; V.V.V. contributed to conceptualization/study design, methodology, supervision, direction of data analysis and manuscript preparation, and funding support acquisition.

DECLARATION OF INTERESTS

The authors declare no competing interests.

STAR★METHODS

Detailed methods are provided in the online version of this paper and include the following:

- KEY RESOURCES TABLE
- EXPERIMENTAL MODEL AND SUBJECT DETAILS
  - Animals and housing conditions

SUPPLEMENTAL INFORMATION

Supplemental information can be found online at https://doi.org/10.1016/j.cub.2025.02.053.

Received: August 14, 2023
Revised: December 10, 2024
Accepted: February 25, 2025
Published: March 20, 2025

REFERENCES

1. Banks, G.T., Guillaumin, M.C.C., Heise, I., Lau, P., Yin, M., Bourbia, N., Aguilar, C., Bowl, M.R., Esapa, C., Brown, L.A., et al. (2020). Forward genetics identifies a novel sleep mutant with sleep state inertia and REM sleep deficits. Sci. Adv. *6*, eabb3567.
2. Massimini, M., Huber, R., Ferrarelli, F., Hill, S., and Tononi, G. (2004). The sleep slow oscillation as a traveling wave. J. Neurosci. *24*, 6862–6870.
3. Steriade, M., McCormick, D.A., and Sejnowski, T.J. (1993). Thalamocortical oscillations in the sleeping and aroused brain. Science *262*, 679–685.
4. Borbély, A.A., Tobler, I., and Hanagasioglu, M. (1984). Effect of sleep deprivation on sleep and EEG power spectra in the rat. Behav. Brain Res. *14*, 171–182.
5. Achermann, P., and Borbély, A.A. (2003). Mathematical models of sleep regulation. Front. Biosci. *8*, s683–s693.
6. Borbély, A.A., Baumann, F., Brandeis, D., Strauch, I., and Lehmann, D. (1981). Sleep deprivation: effect on sleep stages and EEG power density in man. Electroencephalogr. Clin. Neurophysiol. *51*, 483–495.
7. Dijk, D.J., Beersma, D.G., and Daan, S. (1987). EEG power density during nap sleep: reflection of an hourglass measuring the duration of prior wakefulness. J. Biol. Rhythms *2*, 207–219.
8. Calvet, J., Fourment, A., and Thiefry, M. (1973). Electrical activity in neocortical projection and association areas during slow wave sleep. Brain Res. *52*, 173–187.
9. Contreras, D., and Steriade, M. (1995). Cellular basis of EEG slow rhythms: a study of dynamic corticothalamic relationships. J. Neurosci. *15*, 604–622.
10. Steriade, M., Timofeev, I., and Grenier, F. (2001). Natural waking and sleep states: a view from inside neocortical neurons. J. Neurophysiol. *85*, 1969–1985.
11. Mukovski, M., Chauvette, S., Timofeev, I., and Volgushev, M. (2007). Detection of active and silent states in neocortical neurons from the field potential signal during slow-wave sleep. Cereb. Cortex *17*, 400–414.
12. Vyazovskiy, V.V., Olcese, U., Lazimy, Y.M., Faraguna, U., Esser, S.K., Williams, J.C., Cirelli, C., and Tononi, G. (2009). Cortical firing and sleep homeostasis. Neuron *63*, 865–878.
13. Harding, C.D., Guillaumin, M.C.C., Krone, L.B., Kahn, M.C., Blanco-Duque, C., Mikutta, C., and Vyazovskiy, V.V. (2023). Detection of neuronal OFF periods as low amplitude neural activity segments. BMC Neurosci. *24*, 13.
14. Neckelmann, D., and Ursin, R. (1993). Sleep stages and EEG power spectrum in relation to acoustical stimulus arousal threshold in the rat. Sleep *16*, 467–477.
15. Nir, Y., Vyazovskiy, V.V., Cirelli, C., Banks, M.I., and Tononi, G. (2015). Auditory responses and stimulus-specific adaptation in rat auditory cortex are preserved across NREM and REM sleep. Cereb. Cortex *25*, 1362–1378.
16. Rechtschaffen, A., Hauri, P., and Zeitlin, M. (1966). Auditory awakening thresholds in REM and NREM sleep stages. Percept. Mot. Skills *22*, 927–942.
17. Hayat, H., Marmelshtein, A., Krom, A.J., Sela, Y., Tankus, A., Strauss, I., Fahoum, F., Fried, I., and Nir, Y. (2022). Reduced neural feedback signaling despite robust neuron and gamma auditory responses during human sleep. Nat. Neurosci. *25*, 935–943.
18. Wimmer, R.D., Astori, S., Bond, C.T., Rovó, Z., Chatton, J.Y., Adelman, J.P., Franken, P., and Lüthi, A. (2012). Sustaining sleep spindles through enhanced SK2-channel activity consolidates sleep and elevates arousal threshold. J. Neurosci. *32*, 13917–13928.
19. Guillaumin, M.C.C., McKillop, L.E., Cui, N., Fisher, S.P., Foster, R.G., de Vos, M., Peirson, S.N., Achermann, P., and Vyazovskiy, V.V. (2018). Cortical region-specific sleep homeostasis in mice: effects of time of day and waking experience. Sleep *41*, zsy079.
20. Thomas, C.W., Guillaumin, M.C., McKillop, L.E., Achermann, P., and Vyazovskiy, V.V. (2020). Global sleep homeostasis reflects temporally and spatially integrated local cortical neuronal activity. eLife *9*, e54148.
21. Sanchez-Vives, M.V., Massimini, M., and Mattia, M. (2017). Shaping the Default Activity Pattern of the Cortical Network. Neuron *94*, 993–1001.
22. Sanchez-Vives, M.V., and Mattia, M. (2014). Slow wave activity as the default mode of the cerebral cortex. Arch. Ital. Biol. *152*, 147–155.
23. Bandarabadi, M., Vassalli, A., and Tafti, M. (2020). Sleep as a default state of cortical and subcortical networks. Curr. Opin. Physiol. *15*, 60–67.
24. Buzsáki, G. (2006). The Brain's Default State: Self-Organized Oscillations in Rest and Sleep. In Rhythms of the Brain, Online Edition (Oxford Academic).
25. Lemieux, M., Chen, J.Y., Lonjers, P., Bazhenov, M., and Timofeev, I. (2014). The impact of cortical deafferentation on the neocortical slow oscillation. J. Neurosci. *34*, 5689–5703.
26. Timofeev, I., Schoch, S.F., LeBourgeois, M.K., Huber, R., Riedner, B.A., and Kurth, S. (2020). Spatio-temporal properties of sleep slow waves and implications for development. Curr. Opin. Physiol. *15*, 172–182.
27. Jewett, K.A., Taishi, P., SenGupta, P., Roy, S., Davis, C.J., and Krueger, J.M. (2015). Tumor necrosis factor enhances the sleep-like state and electrical stimulation induces a wake-like state in co-cultures of neurons and glia. Eur. J. Neurosci. *42*, 2078–2090.
28. Krueger, J.M., Nguyen, J.T., Dykstra-Aiello, C.J., and Taishi, P. (2019). Local sleep. Sleep Med. Rev. *43*, 14–21.
29. Brown, E.N., Lydic, R., and Schiff, N.D. (2010). General anesthesia, sleep, and coma. N. Engl. J. Med. *363*, 2638–2650.
30. Clark, D.L., and Rosner, B.S. (1973). Neurophysiologic effects of general anesthetics. I. The electroencephalogram and sensory evoked responses in man. Anesthesiology *38*, 564–582.
31. Shanker, A., Abel, J.H., Schamberg, G., and Brown, E.N. (2021). Etiology of Burst Suppression EEG Patterns. Front. Psychol. *12*, 673529.
32. Huang, Y.G., Flaherty, S.J., Pothecary, C.A., Foster, R.G., Peirson, S.N., and Vyazovskiy, V.V. (2021). The relationship between fasting-induced torpor, sleep, and wakefulness in laboratory mice. Sleep *44*, zsab093.
33. McKillop, L.E., Fisher, S.P., Cui, N.Y., Peirson, S.N., Foster, R.G., Wafford, K.A., and Vyazovskiy, V.V. (2018). Effects of Aging on Cortical Neural Dynamics and Local Sleep Homeostasis in Mice. J. Neurosci. *38*, 3911–3928.
34. Achermann, P., Dijk, D.J., Brunner, D.P., and Borbély, A.A. (1993). A model of human sleep homeostasis based on EEG slow-wave activity: quantitative comparison of data and simulations. Brain Res. Bull. *31*, 97–113.

35. Pimentel, D., Donlea, J.M., Talbot, C.B., Song, S.M., Thurston, A.J.F., and Miesenböck, G. (2016). Operation of a homeostatic sleep switch. Nature *536*, 333–337.

36. Saper, C.B., Fuller, P.M., Pedersen, N.P., Lu, J., and Scammell, T.E. (2010). Sleep state switching. Neuron *68*, 1023–1042.

37. Lu, J., Sherman, D., Devor, M., and Saper, C.B. (2006). A putative flip-flop switch for control of REM sleep. Nature *441*, 589–594.

38. Saper, C.B., Chou, T.C., and Scammell, T.E. (2001). The sleep switch: hypothalamic control of sleep and wakefulness. Trends Neurosci. *24*, 726–731.

39. Funato, H., Miyoshi, C., Fujiyama, T., Kanda, T., Sato, M., Wang, Z., Ma, J., Nakane, S., Tomita, J., Ikkyu, A., et al. (2016). Forward-genetics analysis of sleep in randomly mutagenized mice. Nature *539*, 378–383.

40. Honda, T., Fujiyama, T., Miyoshi, C., Ikkyu, A., Hotta-Hirashima, N., Kanno, S., Mizuno, S., Sugiyama, F., Takahashi, S., Funato, H., et al. (2018). A single phosphorylation site of SIK3 regulates daily sleep amounts and sleep need in mice. Proc. Natl. Acad. Sci. USA *115*, 10458–10463.

41. Jagannath, A., Taylor, L., Ru, Y., Wakaf, Z., Akpobaro, K., Vasudevan, S., and Foster, R.G. (2023). The multiple roles of salt-inducible kinases in regulating physiology. Physiol. Rev. *103*, 2231–2269.

42. Hinard, V., Mikhail, C., Pradervand, S., Curie, T., Houtkooper, R.H., Auwerx, J., Franken, P., and Tafti, M. (2012). Key electrophysiological, molecular, and metabolic signatures of sleep and wakefulness revealed in primary cortical cultures. J. Neurosci. *32*, 12506–12517.

43. Aeschbach, D., Cajochen, C., Landolt, H., and Borbély, A.A. (1996). Homeostatic sleep regulation in habitual short sleepers and long sleepers. Am. J. Physiol. *270*, R41–R53.

44. Piltz, S.H., Diniz Behn, C.G., and Booth, V. (2020). Habitual sleep duration affects recovery from acute sleep deprivation: A modeling study. J. Theor. Biol. *504*, 110401.

45. Krone, L.B., Yamagata, T., Blanco-Duque, C., Guillaumin, M.C.C., Kahn, M.C., van der Vinne, V., McKillop, L.E., Tam, S.K.E., Peirson, S.N., Akerman, C.J., et al. (2021). A role for the cortex in sleep-wake regulation. Nat. Neurosci. *24*, 1210–1215.

46. Antkowiak, B. (2002). In vitro networks: cortical mechanisms of anaesthetic action. Br. J. Anaesth. *89*, 102–111.

47. Lukatch, H.S., and MacIver, M.B. (1996). Synaptic mechanisms of thiopental-induced alterations in synchronized cortical activity. Anesthesiology *84*, 1425–1434.

48. Herring, B.E., Xie, Z., Marks, J., and Fox, A.P. (2009). Isoflurane inhibits the neurotransmitter release machinery. J. Neurophysiol. *102*, 1265–1273.

49. Xie, Z., McMillan, K., Pike, C.M., Cahill, A.L., Herring, B.E., Wang, Q., and Fox, A.P. (2013). Interaction of anesthetics with neurotransmitter release machinery proteins. J. Neurophysiol. *109*, 758–767.

50. Vyazovskiy, V.V., Tobler, I., and Winsky-Sommerer, R. (2007). Alteration of behavior in mice by muscimol is associated with regional electroencephalogram synchronization. Neuroscience *147*, 833–841.

51. Joiner, W.J., Friedman, E.B., Hung, H.T., Koh, K., Sowcik, M., Sehgal, A., and Kelz, M.B. (2013). Genetic and Anatomical Basis of the Barrier Separating Wakefulness and Anesthetic-Induced Unresponsiveness. PLoS Genet. *9*, e1003605.

52. Krishnan, K.S., and Nash, H.A. (1990). A genetic study of the anesthetic response: mutants of *Drosophila Melanogaster* altered in sensitivity to halothane. Proc. Natl. Acad. Sci. USA *87*, 8632–8636.

53. Flourakis, M., Kula-Eversole, E., Hutchison, A.L., Han, T.H., Aranda, K., Moose, D.L., White, K.P., Dinner, A.R., Lear, B.C., Ren, D.J., et al. (2015). A Conserved Bicycle Model for Circadian Clock Control of Membrane Excitability. Cell *162*, 836–848.

54. Franks, N.P. (2008). General anaesthesia: From molecular targets to neuronal pathways of sleep and arousal. Nat. Rev. Neurosci. *9*, 370–386.

55. Pal, D., Lipinski, W.J., Walker, A.J., Turner, A.M., and Mashour, G.A. (2011). State-specific Effects of Sevoflurane Anesthesia on Sleep Homeostasis Selective Recovery of Slow Wave but Not Rapid Eye Movement Sleep. Anesthesiology *114*, 302–310.

56. Tung, A., Szafran, M.J., Bluhm, B., and Mendelson, W.B. (2002). Sleep deprivation potentiates the onset and duration of loss of righting reflex induced by propofol and isoflurane. Anesthesiology *97*, 906–911.

57. Baker, R., Gent, T.C., Yang, Q., Parker, S., Vyssotski, A.L., Wisden, W., Brickley, S.G., and Franks, N.P. (2014). Altered activity in the central medial thalamus precedes changes in the neocortex during transitions into both sleep and propofol anesthesia. J. Neurosci. *34*, 13326–13335.

58. Gelegen, C., Miracca, G., Ran, M.Z., Harding, E.C., Ye, Z., Yu, X., Tossell, K., Houston, C.M., Yustos, R., Hawkins, E.D., et al. (2018). Excitatory Pathways from the Lateral Habenula Enable Propofol-Induced Sedation. Curr. Biol. *28*, 580–587.e5.

59. Steinberg, E.A., Wafford, K.A., Brickley, S.G., Franks, N.P., and Wisden, W. (2015). The role of K_2p channels in anaesthesia and sleep. Pflugers Arch. *467*, 907–916.

60. Nir, Y., and de Lecea, L. (2023). Sleep and vigilance states: Embracing spatiotemporal dynamics. Neuron *111*, 1998–2011.

61. Bréant, B.J., Mengual, J.P., Bannerman, D.M., Sharp, T., and Vyazovskiy, V.V. (2022). "Paradoxical wakefulness" induced by psychedelic 5-methoxy-N,N-dimethyltryptamine in mice. Preprint at bioRxiv.

62. Jang, R.S., Ciliberti, D., Mankin, E.A., and Poe, G.R. (2022). Recurrent Hippocampo-neocortical sleep-state divergence in humans. Proc. Natl. Acad. Sci. USA *119*, e2123427119.

63. Vanderwolf, C.H., and Robinson, T.E. (1981). Reticulo-cortical activity and behavior: A critique of the arousal theory and a new synthesis. Behav. Brain Sci. *4*, 459–476.

64. Vyazovskiy, V.V., and Tobler, I. (2012). The temporal structure of behaviour and sleep homeostasis. PLoS One *7*, e50677.

65. Fisher, S.P., Cui, N., McKillop, L.E., Gemignani, J., Bannerman, D.M., Oliver, P.L., Peirson, S.N., and Vyazovskiy, V.V. (2016). Stereotypic wheel running decreases cortical activity in mice. Nat. Commun. *7*, 13138.

66. Scheller, R.H. (2013). In search of the molecular mechanism of intracellular membrane fusion and neurotransmitter release. Nat. Med. *19*, 1232–1235.

67. Yamagata, T., Kahn, M.C., Prius-Mengual, J., Meijer, E., Šabanović, M., Guillaumin, M.C.C., van der Vinne, V., Huang, Y.G., McKillop, L.E., Jagannath, A., et al. (2021). The hypothalamic link between arousal and sleep homeostasis in mice. Proc. Natl. Acad. Sci. USA *118*, e2101580118.

68. Banks, G., Nolan, P.M., and Peirson, S.N. (2016). Reciprocal interactions between circadian clocks and aging. Mamm. Genome *27*, 332–340.

STAR★METHODS

KEY RESOURCES TABLE

REAGENT or RESOURCE	SOURCE	IDENTIFIER
Chemicals, peptides, and recombinant proteins		
ProLong Glass Antifade mountant with NucBlue	ThermoFisher Scientific	Cat#: P36981
1,1'-Dioctadecyl-3,3,3',3'-Tetramethylindocarbocyanine Perchlorate dye	ThermoFisher Scientific	Cat#: D3911
Kwik-Sil	World Precision Instruments	N/A
Experimental models: Organisms/strains		
rlss colony (Vamp2^{rlss}, C3H.Pde6b+ background)	MRC Harwell; Banks et al.[1]	MGI:5792085
Software and algorithms		
SPSS, Release 23.0.0.2	IBM Corp.	RRID:SCR_019096; https://www.ibm.com/products/spss-statistics
Matlab, version R2019b	The MathWorks Inc.	RRID:SCR_001622; https://uk.mathworks.com/products/matlab.html
Synapse software	Tucker-Davis Technologies	https://www.tdt.com/docs/synapse/
SleepSign software	Kissei Comtec Co	RRID:SCR_018200; http://www.sleepsign.com
OFF-period detection algorithm (OFFAD)	Harding et al.[13]	https://github.com/sjoh4302/OFFAD
Other		
RM3 diet (E) (FG), expanded and fine-ground	Special Diets Services	https://www.sds-diets.com/sds_en/products/rodent.php
Laminar probes type A1x16-3mm-100-703-Z16	NeuroNexus Technologies	N/A

EXPERIMENTAL MODEL AND SUBJECT DETAILS

Animals and housing conditions

All work was carried out in accordance with the UK Animal [Scientific Procedures] Act 1986 and the University of Oxford's Policy on the Use of Animals in Scientific Research, and in compliance with the Animal Research: Reporting In Vivo Experiments (ARRIVE) guidelines. Mice from the *rlss* colony (MGI:5792085, C3H.Pde6b+ background) were initially obtained from MRC Harwell (U.K.) and were then bred in-house. N=5 *rlss* homozygotes and n=5 WT littermates (all males) were implanted. The experimenter was not blind to the animals' genotype. Over the two months preceding surgeries, to promote weight gain, *rlss* homozygote mice were fed a high-nutrient diet (RM3 diet, ground, Special Diets Services, U.K.) in the form of mash in addition to the regular pellets. Mice were implanted once they had reached a weight nearing or above 30g, which meant that mice were overall 9 weeks older at surgery. The average age and weight of the animals at the time of surgery was 23.8 ± 1.2 weeks & 31.9 ± 0.8 g for the homozygotes and 14.7 ± 1.5 weeks & 31.7 ± 1.5 g for the WT mice. Age differences were permitted so that animals were matched by weight. Previous data indicates that this age difference does not contribute to the differences in sleep observed.[33,68]

METHOD DETAILS

EEG and laminar probe implantation surgeries

On the day preceding surgery, mice were injected with Dexamethasone (0.2 mg/kg, subcutaneous route). Surgeries were performed using aseptic techniques under isoflurane anaesthesia (1-2%). Mice were provided with meloxicam (5 mg/kg s.c.), buprenorphine (0.1 mg/kg) and Dexamethasone (0.2 mg/kg) prior to surgery start. Screws (self-tapping bone screws, stainless steel, length: 4 mm, shaft diameter: 0.85 mm, Fine Science Tools Inc.) were positioned (Motor cortical area (frontal): AP +2 mm, ML +2 mm; Visual cortical area (occipital): AP -3.5 mm, ML + 2.5 mm; Cerebellum: 2 mm behind lambda; Anchor screw: AP -3.5 mm, ML -2.5 mm). Frontal EEG signals are well suited to measure SWA and detect spindles, while occipital EEG signals are better suited to investigate theta activity, active wakefulness and REMS. A small craniotomy was performed around the laminar probe (type A1x16-3mm-100-703-Z16, NeuroNexus Technologies, Ann Arbor, USA) insertion point (≈0.8mm x 0.8 mm, primary motor cortex, AP +1.1, ML -1.75, DV 1.8, tilt of 14°). The tip of the electrode was dyed prior to the surgery with 1,1'-Dioctadecyl-3,3,3',3'-Tetramethylindocarbocyanine Perchlorate dye ('DiI', ThermoFisher Scientific). The probe was grounded to the anchor screw and referenced to the cerebellar screw and carefully lowered into the cortex (1.8 mm from

the point at which the tip touches the surface of the brain). Silicon gel (Kwik-Sil, World Precision Instruments, USA) was applied on the craniotomy and the implant cemented. Two electromyography (EMG) electrodes were inserted in the neck muscle and fixed to the back of the head cap with dental cement. Saline was injected subcutaneously (0.1 mL/20 g) to compensate for fluid loss during the duration of the surgery, before placing the mouse in a recovery chamber at 28°C. Animals were administered with Dexamethasone (0.2 mg/kg, s.c.) and meloxicam (5 mg/kg, s.c.) for 1 and 3 days following surgery, respectively.

Recordings and initial data processing

Animals were left to recover for at least 2 weeks before being moved to custom-made clear plexiglas cages (20.3 x 32 x 35 cm^3) placed in ventilated, sound-attenuated Faraday chambers (Campden Instruments, UK). Mice were kept in a 12h:12h light-dark cycle (lights on at 9am), with water and food available ad libitum. Temperature within the room was kept at 22±2 °C, with a humidity level of 55±10 %, and light levels of 120-180 lux.

Mice were left to habituate to their new environment for 3 days before being tethered. Recordings were started at least 3 days after tethering, to let the mice habituate to the cables. Signals were recorded using the Multichannel Neurophysiology Recording System (TDT, USA) and the Synapse software (TDT, USA). As described earlier,[1] EEG and EMG signals were filtered (0.1–100 Hz), amplified (PZ5 NeuroDigitizer preamplifier, Tucker-Davis Technologies) and stored at a sampling rate of 256.9 Hz. Signals were extracted and converted using custom-written Matlab (The MathWorks Inc., USA) scripts as previously described.[19,33] Vigilance states – wake, NREMS, REMS, or brief awakenings (short arousals $\leq$16 sec during sleep, as described previously[12]) – were scored manually using the SleepSign software (Kissei Comtec Co, Nagano, Japan). In brief, data was scored in 4-s epochs. Epochs with low-amplitude, high-frequency EEG and a high level of EMG were scored as wake. Those presenting slow-waves, and high-amplitude, low-frequency EEG concomitant with low levels of EMG activity were defined as NREMS. Epochs with low-amplitude, high-frequency EEG with a low level of EMG activity were scored as REMS. Finally, if the visualized LFP or EEG channels were contaminated with artifacts (while still being scorable) the epoch was scored as artefactual (i.e. the vigilance state was defined and included in quantification of time spent in each state, but the signals from such an epoch were not included in signal-based analyses). EEG power density spectra were computed by a Fast Fourier Transform (Hanning window; 0.25-Hz resolution). More detailed recording and initial analysis methods were as previously published.[1,33,68] As the focus of the present study was on the slower frequencies, spectra only show power for frequencies up to 20 Hz.

Sleep deprivation

Sleep deprivation (SD) was performed for 6 consecutive hours starting from light onset (ZT0). Animals were kept awake by providing them with new objects to explore. If the mice were getting drowsy, nesting material was taken away from the cage temporarily. SD was successful as only 7.8 ± 1.7 minutes (mean ± SEM) of sleep were detected during the 6 h of SD. Following sleep deprivation, mice were left undisturbed for at least 18 h.

Auditory stimulation

Sounds of 8kHz, 75dB were played for 8 sec every minute during 1h30 (90 repetitions of 8-sec sound, 52-sec silence). This 1h30 session was performed 4 times across 24 h: ZT 0.5 – 2; ZT 7.5 – 9; ZT 12.5 – 14; ZT 20 – 21.5. Speakers were placed 70 cm above each animal, within the Faraday sound-attenuated chambers.

Detection of OFF-periods

Detection of low-amplitude neural activity segments ('OFF-periods') was performed using the GUI made available by C. Harding, described in Harding et al.[13] Default parameters of the GUI were used for OFF-period detection (Calinski-Harabasz clustering evaluation method; Clustering variable 1: amplitude, 15 smoothing points; clustering variable 2: amplitude, 5 smoothing points; clustering sample size: 1%). Out of the 16 channels, 5-10 MUA channels (and corresponding LFP channel for visualization) were selected for each mouse, selecting only those that were stable across a 48h (baseline day + sleep deprivation day). The first 12 h of the baseline day were used as a new dataset against which the detection parameters were calculated for each mouse. The parameters ('pre-sets') were then re-used to detect OFF-periods for the next 36 h of recording.

In some instances (specified in the legends and text), only the 5% longest OFF periods were included. The 5% threshold was chosen to include enough OFF periods, while still focusing on the longest ones, wherever that was the focus of our investigations. Other criteria were tested (1% longest OFF-periods, 5% percentile value of OFF-period duration) with little effect on the outcome – i.e. effects observed were robust to the variations in criterion used.

Application of the 'elaborated two-process model'

The estimation and optimisation of the model parameters (gain constant gc, describing the decay rate of SWA; rise constant rs and upper asymptote S_U) were performed exactly as described in Guillaumin et al.,[19] using SWA calculated across a 24-h baseline day and a sleep deprivation day (6-h sleep deprivation + 18-h recovery sleep). For the baseline-only optimisations, the baseline recordings were artificially duplicated for the estimation/optimisation of the parameters, as described in the above-mentioned publication.

For the BL+SD day, the 24-h baseline day followed by the sleep deprivation day were used. The equations, identical to Guillaumin et al.,[19] are replicated here:

(1) Slow-wave activity (SWA(t)):

Empirical SWA (and therefore simulated SWA) is always expressed – unless otherwise stated – as a percentage of mean SWA across NREMS in the baseline period used for optimisations.

$$\frac{dSWA}{dt} = rc.SWA.\frac{S}{SU}.\left(1 - \frac{SWA}{S}\right).(1 - WT(t)).(1 - REMT(t))$$

$$- fc_R.\,(SWA - SWA_L).\,REMT(t)$$

$$- fc_W.\,(SWA - SWA_L).\,WT(t)$$

(2) REMS (REMT(t)):

$$REMT(t) = \begin{cases} 1\ during\ REMS'trigger' \\ 0\ otherwise \end{cases}$$

(3) Waking (WT(t)):

$$WT(t) = \begin{cases} 1\ during\ wake'trigger' \\ 0\ otherwise \end{cases}$$

(4) Process S (S(t)):

$$\frac{ds}{dt} = -gc.SWA + (S_U - S).rs$$

Perfusions and micro-lesions

Mice were injected with Pentobarbital (200mg in 1 mL, i.p. injection of 0.01mL/g body weight). Microlesions of 3 selected channels on the laminar probe were then performed using a NanoZ device (White Matter) before the mice were transcardially perfused with a PBS solution, followed by paraformaldehyde (PFA, 4% in PBS). Brains were removed and placed in PFA (4% in PBS) for 48 h, after which they were transferred to a 30% sucrose solution (in PBS) for cryoprotection. Once sunk to the bottom of the vial, brains were briefly rinsed in PBS and embedded in O.C.T. compound and frozen at -80°C until cutting.

Histology

To confirm electrode placement, slices were prepared using a cryostat (Cryotome FSE, ThermoScientific; -22°C, 50μm-thick sections) and mounted on glass slides. Slides were subsequently mounted under cover glasses with ProLong Glass Antifade mountant with NucBlue stain (ThermoFisher Scientific). Sections were digitized using an LSM 710 laser scanning confocal microscope and ZEN image acquisition software (Zeiss) (Figure S6C).

QUANTIFICATION AND STATISTICAL ANALYSIS

All statistical analyses were performed using SPSS (IBM Corp., Release 23.0.0.2) and Matlab (The MathWorks Inc., USA). The nature of the tests used and corresponding results are reported within figure legends or within the main text of the results section. Wilcoxon rank sum test was used where normality was not observed (Kolmogorov Smirnov test).

For the OFF-period duration survival curves fitting, we computed survival curves for data associated with each mouse and channel during the baseline light phase. On the semilog plot, survival curves were approximately linear. Therefore, we fit lines to the survival curves for each mouse and each channel. We computed the average slope for each mouse and compared between groups with ANOVA. Deviations from the linear fits tended to occur at the beginning of the survival curve and corresponded to OFF-periods with shorter durations; therefore, we separately compared the slopes of fits to the survival curves for subsets of OFF-period data with durations greater than a fixed threshold, and we varied the threshold between 5 and 200 ms to identify the subsets of OFF-period data for which slopes were different. We also applied Levene's test to compare variances of slopes between groups.